

 Open access • Journal Article • DOI:10.1103/PHYSREVA.19.1169

Theoretical and experimental study of the dynamic behavior of a nonlinear Fabry-Perot interferometer — [Source link](#)

T. Bischofberger, Y. R. Shen

Institutions: University of California, Berkeley

Published on: 01 Mar 1979 - Physical Review A (American Physical Society)

Topics: Switching time, Overshoot (signal), Response time and Kerr effect

Related papers:

- [Differential Gain and Bistability Using a Sodium-Filled Fabry-Perot Interferometer](#)
- [Theory of a lossless nonlinear Fabry-Perot interferometer](#)
- [Theory of nonresonant multistable optical devices](#)
- [Optical Turbulence: Chaotic Behavior of Transmitted Light from a Ring Cavity](#)
- [Cooperative effects and bistability for resonance fluorescence](#)

Share this paper:    

View more about this paper here: <https://typeset.io/papers/theoretical-and-experimental-study-of-the-dynamic-behavior-480if59pck>

Lawrence Berkeley National Laboratory

Recent Work

Title

THEORETICAL AND EXPERIMENTAL STUDY OF THE DYNAMIC BEHAVIOR OF A NONLINEAR FABRY-PEROT INTERFERROMETER

Permalink

<https://escholarship.org/uc/item/51n0k66z>

Author

Bischofberger, T.

Publication Date

1978-09-01

Submitted to Physical Review

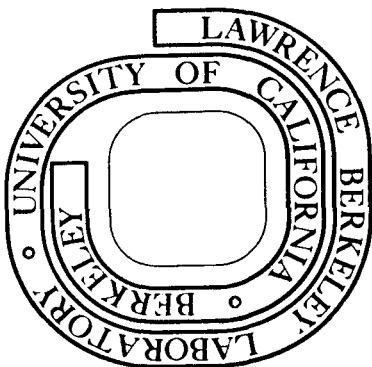
LBL-8179 c.2
Preprint

THEORETICAL AND EXPERIMENTAL STUDY OF THE DYNAMIC BEHAVIOR
OF A NONLINEAR FABRY-PEROT INTERFERROMETER

T. Bischofberger and Y. R. Shen

September 1978

Prepared for the U. S. Department of Energy
under Contract W-7405-ENG-48



TWO-WEEK LOAN COPY

*This is a Library Circulating Copy
which may be borrowed for two weeks.
For a personal retention copy, call
Tech. Info. Division, Ext. 6782*

LBL-8179
c.2

DISCLAIMER

This document was prepared as an account of work sponsored by the United States Government. While this document is believed to contain correct information, neither the United States Government nor any agency thereof, nor the Regents of the University of California, nor any of their employees, makes any warranty, express or implied, or assumes any legal responsibility for the accuracy, completeness, or usefulness of any information, apparatus, product, or process disclosed, or represents that its use would not infringe privately owned rights. Reference herein to any specific commercial product, process, or service by its trade name, trademark, manufacturer, or otherwise, does not necessarily constitute or imply its endorsement, recommendation, or favoring by the United States Government or any agency thereof, or the Regents of the University of California. The views and opinions of authors expressed herein do not necessarily state or reflect those of the United States Government or any agency thereof or the Regents of the University of California.

DISCLAIMER

This document was prepared as an account of work sponsored by the United States Government. While this document is believed to contain correct information, neither the United States Government nor any agency thereof, nor the Regents of the University of California, nor any of their employees, makes any warranty, express or implied, or assumes any legal responsibility for the accuracy, completeness, or usefulness of any information, apparatus, product, or process disclosed, or represents that its use would not infringe privately owned rights. Reference herein to any specific commercial product, process, or service by its trade name, trademark, manufacturer, or otherwise, does not necessarily constitute or imply its endorsement, recommendation, or favoring by the United States Government or any agency thereof, or the Regents of the University of California. The views and opinions of authors expressed herein do not necessarily state or reflect those of the United States Government or any agency thereof or the Regents of the University of California.

THEORETICAL AND EXPERIMENTAL STUDY OF THE DYNAMIC BEHAVIOR
OF A NONLINEAR FABRY-PEROT INTERFERROMETER

T. Bischofberger[†] and Y. R. Shen^{*}
Physics Department, University of California
Berkeley, California 94720

and

Materials and Molecular Research Division
Lawrence Berkeley Laboratory
Berkeley, California 94720

September 1978

ABSTRACT

We have studied theoretically and experimentally the dynamic behavior of a nonlinear Fabry-Perot filled with a Kerr medium. The Fabry-Perot responses ranging from extremely transient to quasi-steady-state in various modes of operation are considered. The experimental results are in excellent agreement with theory. It is shown that the quasi-steady-state operation requires not only a medium response time much smaller than the cavity round-trip time, but also a characteristic time of the input intensity variation several hundred times larger than the cavity round-trip time. Even in the quasi-steady-state limit, optical switching is often featured by overshoot and ringing after switching. The switching speed is limited by the cavity buildup time.

[†]Supported by the Division of Materials Sciences, Office of Basic Energy Sciences, U.S. Department of Energy.
Present address: Solid State Physics Laboratory, Swiss Federal Institute of Technology (ETH), CH-8093, Zurich, Switzerland

^{*}Supported by National Science Foundation Grant No. 444010-21862

I. Introduction

Recently, there has been growing interest in the physical understanding and possible applications of nonlinear Fabry-Perot (FP).¹ Seidel and Szoke et al. first proposed the use of a nonlinear absorbing FP for optical limiting, discriminator, and bistable operations.² Later, McCall and coworkers successfully demonstrated such operations with sodium vapor or ruby as the nonlinear medium in the FP cavity.³ They noticed, however, that their observations were actually dominated by the field-induced refractive index rather than the nonlinear absorption. Detailed theory of the steady-state operation of a nonlinear FP filled with a purely refractive medium has already been worked out by Felber and Marburger.⁴ More recently, various research groups have proposed and developed schemes that could lead to miniature nonlinear FP for applications in integrated optical circuits.⁵ Even mirrorless and integrated optical bistable devices have been demonstrated.⁶ Theoretically, optical bistability has been discussed using analog to phase transition.⁷ The quantum statistical properties and the spectrum of transmitted light of a bistable resonator have also been investigated.⁸

While the steady-state operation of a nonlinear FP is now well understood, little attention, so far, has been paid to the dynamic behavior of a nonlinear FP. In the practical design of a nonlinear FP as an optical device, however, questions relating to the transient characteristics of the device, switching speed, etc. are clearly very important. We have recently reported the preliminary results of our theoretical and experimental study of the transient behavior of a nonlinear FP filled with a Kerr liquid.⁹ In this paper, we now give a complete theoretical analysis on

how the nonlinear FP behaves in its operation from the extremely transient case to the quasi-steady-state case as different characteristic parameters are varied.¹⁰ We also show experimentally that our results obtained with an FP filled with various Kerr media (liquid crystal, nitrobenzene, and CS₂) are in excellent agreement with the theoretical calculations.

We first review in Sec. II the theoretical formalism. We then describe, in Sec. III, the experimental arrangement and present, in Sec. IV, the experimental results in comparison with the theoretical calculations. In Sec. V, we extend the theoretical calculations of the bistable operation to the case with an ideal saw-tooth input pulse in order to discuss the transient operation characteristics of the nonlinear FP more fully. We consider, in particular, the dependence of switching speed and ringing in the output on the various characteristic parameters. Finally, we discuss qualitatively the effect of transient response on the observed behavior of the nonlinear FP reported by others.

II. Theoretical Formalism⁹

We consider an FP cavity filled with a Kerr medium. We assume that the field-induced refractive index Δn in the Kerr medium affects only the phase but not the amplitude of the field inside the cavity. Then, in the plane wave approximation with an input field $E_{in}(t) = \mathcal{E}_i(t)\exp(-i\omega t)$, the transmitted output field is

$$\begin{aligned}
 E_{out}(t) &= Te^{-i\omega t} \sum_{m=0}^{\infty} \mathcal{E}_i(t - (m + \frac{1}{2})t_R) R_{\alpha}^m e^{i\phi(t, t - (m + \frac{1}{2})t_R)} \\
 &= Te^{-i\omega t} \sum_{\ell=0}^{\infty} \sum_{m=0}^{\ell} \Delta \mathcal{E}_{i\ell} R_{\alpha}^m e^{i\phi(t, t - (m + \frac{1}{2})t_R)} \quad (1)
 \end{aligned}$$

where $\mathcal{E}_i(t - (m + \frac{1}{2})t_R) = \sum_{\ell=m}^{\infty} \Delta \mathcal{E}_{i\ell}$ with $\Delta \mathcal{E}_{i\ell} = \mathcal{E}_i(t - (\ell + \frac{1}{2})t_R) - \mathcal{E}_i(t - (\ell - \frac{1}{2})t_R)$, ℓ and m are positive integers, t_R is the cavity round trip time, $R_\alpha = R \exp(-\alpha d)$, α is the attenuation coefficient in the cavity, d is the cavity length, R and T are the mirror reflection and transmission coefficients respectively, and $\phi(t, t - (m + \frac{1}{2})t_R)$ is the phase increment of the field entering the cavity at $t - (m + \frac{1}{2})t_R$ and leaving the cavity at t . If the variation of the field is small in t_R , then Eq. (1) can be approximated by

$$E_{\text{out}}(t) = T e^{-i\omega t} \int_{-\infty}^t \left(\frac{d}{dt'} \mathcal{E}_i(t') \right) \sum_{m=0}^{m_{\text{max}}} R_\alpha^m e^{i\phi(t, t - (m + \frac{1}{2})t_R)} dt' \quad (2)$$

with m_{max} being an integer closest to but smaller than $(t - t')/t_R$.

The phase increment ϕ is given by

$$\begin{aligned} \phi(t, t - (m + \frac{1}{2})t_R) = & \sum_{\ell=0}^m (\omega/c) \left\{ \int_0^d [n_o + \Delta n(t - (\ell + \frac{1}{2})t_R + (c/n_o)z, z)] dz \right. \\ & \left. + \sum_{\ell=1}^m (\omega/c) \int_d^0 [n_o + \Delta n(t - \ell t_R + (c/n_o)(d - z), z)] dz \right\} \quad (3) \end{aligned}$$

Assuming the variation of Δn in a round trip time t_R is negligible, we can write

$$\phi(t, t - (m + \frac{1}{2})t_R) \cong (m + \frac{1}{2})\phi_o + \frac{1}{2} \Delta\phi(t) + \sum_{\ell=1}^m \Delta\phi(t - \ell t_R) \quad (4)$$

where $\phi_o = (\omega/c)2n_o d$ and $\Delta\phi(t) = (\omega/c) \oint \Delta n(t, z) dz$. The spatial variation of Δn arises from the interference of the forward and backward propagating waves in the cavity. It is sinusoidal and is therefore averaged

out in the round-trip integral of $\Delta\phi$. For Kerr liquids, Δn and hence $\Delta\phi$ obey the Debye relaxation equation, namely,

$$\tau_D \frac{\partial \Delta\phi}{\partial t} + \Delta\phi = \frac{\omega d}{c} (\delta n_F + \delta n_B) \quad (5)$$

where τ_D is the Debye relaxation time, and δn_F and δn_B are the quasi-steady-state field-induced refractive indices seen by the forward and backward propagating waves E_F and E_B inside the cavity respectively. Since the field-induced polarization in the medium is $P_{F,B}^{(3)} = (n_o/2\pi)n_2(|E_F|^2 + |E_B|^2) \times E_{F,B}$, we have $\Delta n_{F,B} = (2\pi/n_o) \partial P_{F,B}^{(3)} / \partial E_{F,B} = 2n_2 |E_{F,B}|^2 + n_2 |E_{B,F}|^2$. Equation (5) then becomes

$$\tau_D \frac{\partial \Delta\phi}{\partial t} + \Delta\phi = \frac{3\omega d n_2}{c} (|E_F|^2 + |E_B|^2) \quad (6)$$

The fields inside the cavity are related to E_{out} by $|E_{out}|^2 = n_o T |E_F|^2 = n_o T |E_B|^2 / R$. Equation (6) can be written in the integral form as

$$\Delta\phi(t) = \frac{3\omega d n_2 (1+R)}{n_o c T \tau_D} \int_{-\infty}^t |E_{out}(t')|^2 e^{-(t-t')/\tau_D} dt' \quad (7)$$

The coupled set of equations (1), (4), and (7) now fully describe the dynamical property of the nonlinear FP. They can be solved numerically on a computer using iterative, self-consistent loops. A number of examples will be shown in the following sections. When the characteristic time T_c of the input intensity variation is much larger than τ_D and t_R , the operation of the FP should become quasi-steady-state. As expected, Eq. (1) then reduces to the well-known result

$$E_{\text{out}} = TE_{\text{in}} \exp[i(\phi_0 + \Delta\phi)/2] / [1 - R_\alpha \exp(i\phi_0 + i\Delta\phi)] \quad (8)$$

and Eq. (7) becomes

$$\Delta\phi = [3\omega dn_2(1 + R)/n_0 cT] |E_{\text{out}}|^2 \quad (9)$$

In later sections, we shall discuss how large T_c should be relative to τ_D and t_R in order to assure the quasi-steady-state operation.

III. Experimental Arrangement

There are three important time constants in the problem: the characteristic time of input intensity variation T_c , the medium response time τ_D , and the cavity round-trip time t_R (or the cavity buildup time τ_c defined as $\tau_c = t_R / |1 - R_\alpha \exp(i\phi_0)|$). In our experiment, the input to the FP was a laser pulse; so we can use the pulsewidth τ_p as the characteristic time T_c . With the Kerr medium in the FP, τ_D is the Debye relaxation time. We wanted to consider in our experiment cases ranging from $\tau_D \gg \tau_p \gg t_R$ to $\tau_p > \tau_D > t_R$ to $\tau_D \gg \tau_p \gg t_R$, covering a wide range of the non-linear FP operation from the extremely transient to the quasi-steady-state. In order to achieve this, we used three different Kerr media: a liquid crystalline material n-p-methoxybenzylidene-p-butylaniline (MBBA) in the isotropic phase, nitrobenzene, and CS_2 . Because of its pretransitional behavior, MBBA has a relaxation time τ_D which can be easily varied by temperature.¹¹ Corresponding to a temperature variation from 65°C to 45°C, τ_D of MBBA varies from 15 to 174 nsec. Then, for nitrobenzene and CS_2 , we have $\tau_D = 45$ psec and 2 psec at 20°C respectively. We also used

two single-mode Q-switched ruby lasers with different pulsewidths $\tau_p = 14$ nsec and 62 nsec (FWHM) respectively. Both laser beams had a Gaussian beam profile with a radius of ~ 0.15 cm at the entrance of the FP.

Our experimental setup is shown in Fig. 1. The FP cavity was formed by two $\lambda/200$ plane mirrors with $R = 0.98$ separated by $d = 1$ cm. It was filled with one of the Kerr liquids and placed in a thermally controlled oven. The temperature of the FP could be stabilized to within 10^{-3} °C. The linear round-trip phase shift ϕ_0 in the cavity was measured by an He-Ne laser beam and then modified to its value at the ruby laser frequency through calibration. For coarse adjustment of ϕ_0 , the FP was mechanically tuned, and for fine adjustment, thermally tuned. Because of the small attenuation loss due to scattering and absorption in the three Kerr liquids we used, the effective mirror reflectivity at the ruby laser frequency was $R_\alpha \approx 0.78$. The experimentally determined finesse of the FP was 13. Input and output laser pulses at the FP were measured by fast photodiodes and displayed on two simultaneously triggered Tektronix 519 oscilloscopes. The input laser power was always kept well below the self-focusing threshold in the Kerr medium. Absolute laser intensities were obtained by measuring the laser power, the beam cross-section, and the beam divergence at the entrance of the FP. The measured peak laser intensities were accurate to within 15%.

IV. Experimental Results and Comparison to Theory

Our measurements with different pulse intensities were made at FP phase detunings $\Delta\phi_0 = 0, -0.1\pi$, and -0.2π rad ($\phi_0 = \Delta\phi_0 + \text{multiple of } 2\pi$). These values of $\Delta\phi_0$ were chosen such that the steady-state opera-

tion of the nonlinear FP are in three different distinct modes, e.g., the power limiter, the differential gain, and the bistable mode respectively. Figure 2 shows three typical examples for each value of $\Delta\phi_0$. The dots are obtained from the measured oscilloscope traces. The plots on the right-hand side of the figure give I_{out} versus I_{in} with time t as the varying parameter. The solid curves are the theoretical curves. We first fit the measured $I_{in}(t)$ by a Gaussian pulse. Then, using Eqs. (1), (3), and (7), we calculated $I_{out}(t)$ and $\Delta\phi(t)$. The self-consistent calculation was carried out with the difference of $\Delta\phi_0$ between two final successive iteration steps less than 1 milliradian. One normalization constant was used to fit the peak of $I_{out}(t)$ in Fig. 2(a), and then, the same normalization constant was used for calculating $I_{out}(t)$ and $\Delta\phi(t)$ in Figs. 2(b) and (c). Furthermore, the calculated $I_{out}(t)$ also took into account the response time of the detector system through convolution with the detector response function. The same procedure was taken in calculating the curves in Figs. 3-8. In all cases, we find excellent agreement between theory and experiment.

Figures 2-8 show progressively how $I_{out}(t)$, $\Delta\phi(t)$, and $I_{out}(t)$ versus $I_{in}(t)$ vary when the molecular relaxation time τ_D decreases from $\tau_D \gg \tau_p \gg \tau_R$ to $\tau_D \ll \tau_R \ll \tau_p$. When $\tau_D \geq \tau_p$ (Figs. 2-5), the curves of $\Delta\phi(t)$ show clearly the transient response of the medium to the cavity field, but when $\tau_D \ll \tau_p$ (Figs. 6-8), the medium responds to the field almost instantaneously, and $\Delta\phi(t)$ becomes essentially proportional to $I_{out}(t)$. The variation from the transient to the quasi-steady-state operation of the FP can also be easily seen in Figs. 2-8. In the power limiter mode ($\Delta\phi_0 = 0$), I_{out} vs. I_{in} first appears as a loop in the transient case, and gradually

shrinks to a line as the operation becomes less and less transient. In the differential gain mode ($\Delta\phi_0 = -0.1 \pi$ rad.), a similar but more easily visualized transformation takes place with I_{out} vs. I_{in} eventually showing the S-type characteristic curve in the quasi-steady-state limit. The bistable mode of operation ($\Delta\phi_0 = -0.2 \pi$ rad.) displays the transition from transient to quasi-steady-state most dramatically. In the transient limit (Figs. 2(c) and 3(c)), I_{out} vs. I_{in} is also in the form of a loop, even though the circulation around the loop is counter-clockwise, opposite to that appearing in the power limiter and differential gain cases. Then, it begins to appear like a hysteresis loop in Figs. 4(c) and 5(c), and finally transforms into such a loop towards the quasi-steady-state limit in Figs. 6(c)-8(c).

We notice that even in Figs. 6 and 7, with $\tau_p/\tau_D = 310$ and 7000 respectively, the curves exhibit some transient characteristics. This is because in these two cases even though the material response can be considered as instantaneous, $\tau_p/t_R = 140$ is not large enough so that the cavity field buildup is still somewhat transient. With a longer input laser pulse in Fig. 8 corresponding to $\tau_p/t_R = 620$, the transient effect is clearly reduced. Even in the quasi-steady-state, the optical switching of the bistable operation mode occurring in a time comparable to t_R would show some transient phenomenon in the form of overshoot and ringing.⁹ In our experimental observation, however, they are partially masked by the slow response of our detection system. The overshoot and ringing effects could be important in the applications of fast optical switching. We shall therefore discuss theoretically these effects as well as the switching speed in the next section.

V. Dynamic Behavior of Optical Bistability

In order to exhibit more clearly the transient characteristics of the bistable operation, we also performed theoretical calculations using a triangular input pulse. The results are shown in Figs. 9-11 with the detuning of the FP set at $\Delta\phi_0 = -0.4\pi$. In Fig. 9, Three different values of τ_p ($250 t_R$, $100 t_R$, and $50 t_R$) are used while the other parameters such as the Debye relaxation time $\tau_D (= 0.01 t_R)$, the mirror reflectivity $R (= 70\%)$, and the input peak intensity I_{in} (normalized to 1) are kept constant. Since we have $\tau_p > t_R \gg \tau_D$, the medium response in this case is essentially instantaneous. The transient effect therefore arises from the finite time required for the cavity field buildup. As shown in Fig. 9, the transient effect in the sense of slowing down of the switching speed is quite obvious even at $\tau_p/t_R = 100$ and only becomes negligible when $\tau_p/t_R \geq 250$. Then, the overshoot and ringing after switching are also more clearly displayed with longer ringing periods in the more transient cases. Physically, overshoot and ringing after switching can be easily understood. As is well known, field in a resonant cavity cannot make sudden finite changes. It has to approach the final value through interference of multiple reflections. When the finesse (or the Q factor) of the cavity is sufficiently large, we have then the underdamped and ringing situation. We also expect to have more ringing in a cavity with a larger finesse. In the quasi-steady-state with $\tau_p \gg t_R \gg \tau_D$, the ringing should be over in roughly two cavity buildup times (τ_c). If we consider optical switching as completed when the ringing is over, then the switching time is limited by a few τ_c even in the quasi-steady-state operation.

In Fig. 10, we show the effect of the finite medium response time on

the switching behavior. Three examples are given with $\tau_D = 0.01 t_R$, $2.5 t_R$, and $25 t_R$ and the other parameters kept constant. Clearly, even when $\tau_p/\tau_D = 100$, the transient switching characteristic in the form of slow switching and ringing is still obvious. This is mainly because $\tau_D \geq t_R$ so that the material response slows down the cavity field buildup. Therefore, the quasi-steady-state case is expected to set in only when $\tau_D < t_R$ and $\tau_p/\tau_D \geq 250$.

In the quasi-steady-state limit where $\tau_p \gg t_R \gg \tau_D$, the reflectivity of the FP mirrors will finally set the switching speed and affect overshoot and ringing. We show the effect of mirror reflectivity in Fig. 11. As seen in the figure, lower mirror reflectivity slows down the switching speed and damps out the overshoot and ringing. The apparently slower switching is due to the smoother and broader FP transmission curve at lower R, while the stronger damping on the ringing arises from the lower finesse of the cavity.

From the above results, we can therefore conclude that in order to have a sharp optical switching, we need a cavity with a higher finesse, but then overshoot and ringing after switching will be more obvious. The switching speed is fastest in the quasi-steady-state limit ($\tau_p \gg t_R \gg \tau_D$) and is limited by the cavity buildup time.

The theoretical discussion here can be qualitatively extended to the experimental observations reported by others, although the equation governing the material response may be different in different cases. For example, Smith et al.⁵ used a nonlinear FP in which the nonlinear phase shift was provided by an electro-optical crystal driven by the transmitted or reflected light. In that case, the material response was dominated by the re-

sponse time $\tau_F \approx 1$ nsec of the electronic feedback system, i.e., τ_F plays the role of τ_D . Using $\tau_D \equiv \tau_F = 1$ nsec, $t_R \approx 1$ nsec, $R_\alpha \approx 63\%$, and $\tau_p \gg t_R \sim \tau_D$ in our calculation, we can actually obtain a set of I_{out} versus I_{in} curves for the various modes of operation (corresponding to different $\Delta\phi_0$) very similar to what Smith et al. have observed.

Grischkowsky¹² has studied the bistable mode of operation of a nonlinear FP filled with Rb vapor. The characteristic parameters in his case are $t_R = 30$ psec, $\tau_D = 200$ psec, $\tau_p = 7$ nsec, $R_\alpha = 0.73$, and $\Delta\phi_0 = -0.24$ rad. Since $\tau_D > t_R$ even though $\tau_p/t_R = 230 \gg 1$, the transient response of the FP should be quite obvious. The output should resemble the I_{out} curve in Fig. 10(c). An actual calculation taking into account the finite response time (~ 1 nsec) of the detection system and the true input pulse-shape can in fact reproduce the observed $I_{out}(t)$ quite well.

Overshoot and ringing in optical switching of a FP has been mentioned by Smith. They can, in fact, also be seen in the bistable operation of the mirrorless feedback scheme as reported by Feldman.⁶

VI. Conclusion

We have presented here the results of a detailed theoretical and experimental study of the dynamic behavior of a nonlinear FP filled with a Kerr medium. The three modes of operation, namely, power limiter, differential gain, and optical bistability, are considered. The experimental results covering a wide range from the extremely transient to the quasi-steady-state case are all in excellent agreement with theory. We show that in order to have quasi-steady-state operation, the characteristic time of the input intensity variation must be several hundred times the cavity round-trip time which should in turn be larger than the ma-

terial response time. Even in the quasi-steady-state limit, optical switching in the bistable mode of operation is still often characterized by overshoot and ringing as the cavity field makes underdamped adjustment from its initial value to the final value. The optical switching speed is then limited by the cavity buildup time. Switching is less sharp and ringing is more highly damped if the FP cavity has a lower finesse. Although our theoretical calculation is restricted to FP with a Kerr medium, the results are still valid in a qualitative sense for the other types of nonlinear Fabry-Perot.

References

1. See, for example, papers presented in the Xth International Quantum Electronics Conference, Atlanta, Georgia, June 1978.
2. H. Seidel, U.S. Patent No. 3,610,731; A. Szöke, V. Danean, J. Goldhar, and N. A. Kurnit, Appl. Phys. Lett. 15, 376 (1969); A. Szöke, U.S. Patent No. 3,813,605; E. Spiller, J. Appl. Phys. 43, 1673 (1972); J. W. Austin and L. G. DeShazer, J. Opt. Soc. Am. 61, 650 (1971).
3. S. L. McCall, Phys. Rev. A9, 1515 (1974); S. L. McCall, H. M. Gibbs, and T. N. C. Venkatesan, J. Opt. Soc. Am. 65, 1184 (1975); H. M. Gibbs, S. L. McCall, and T. N. C. Venkatesan, Phys. Rev. Lett. 36, 1135 (1976); T. N. C. Venkatesan and S. L. McCall, Appl. Phys. Lett. 30, 282 (1977); H. M. Gibbs, S. L. McCall, and T. N. C. Venkatesan, U.S. Patent No. 4,012,699.
4. F. S. Felber and J. H. Marburger, Appl. Phys. Lett. 28, 731 (1976); J. H. Marburger and F. S. Felber, Phys. Rev. A17, 335 (1978).
5. M. Okuda, M. Togota, and K. Ouaka, Opt. Commun. 19, 138 (1976); M. Okuda and K. Ouaka, Jap. J. Appl. Phys. 16, 769 (1977); P. W. Smith and E. H. Turner, Appl. Phys. Lett. 30, 280 (1977); P. W. Smith, E. H. Turner, and P. J. Maloney, IEEE J. Quant. Elec. QE-14, 207 (1978); P. W. Smith, E. H. Turner, and B. B. Mumford, Optics Lett. 2, 55 (1978).
6. E. Garmire, J. H. Marburger, and S. D. Allen, Appl. Phys. Lett. 32, 320 (1978); A. Feldman, Appl. Phys. Lett. 33, 243 (1978); P. W. Smith, I. P. Kaminow, P. J. Maloney, and L. W. Stulz, Appl. Phys. Lett. 33, 24 (1978).
7. R. Bonafacio and L. A. Luzziato, Optics Comm. 19, 172 (1976); L. M. Narducci and R. Gilmore, in Proceedings of the Fourth Rochester

- Conference on Coherence and Quantum Optics, June 1977, edited by L. Mandel and E. Wolf (Plenum Press, N.Y., to be published); L. A. Luzziato, P. Mandel, S. T. Dembinski, and A. Kossakowski, Phys. Rev. 18, 238 (1978).
8. R. Bonifacio and L. A. Luzziato, Phys. Rev. Lett. 40, 1023 (1978); G. S. Agarwal, L. M. Narducci, D. H. Feng, and R. Gilmore (to be published).
 9. T. Bischofberger and Y. R. Shen, Appl. Phys. Lett. 32, 156 (1978).
 10. Preliminary results were presented in the Xth International Quantum Electronics Conference, Atlanta, Georgia, 1978.
 11. G. K. L. Wong and Y. R. Shen, Phys. Rev. A10, 1277 (1974).
 12. D. Grischkowski, Xth International Quantum Electronics Conference, Atlanta, Georgia, 1978, Paper F.3.

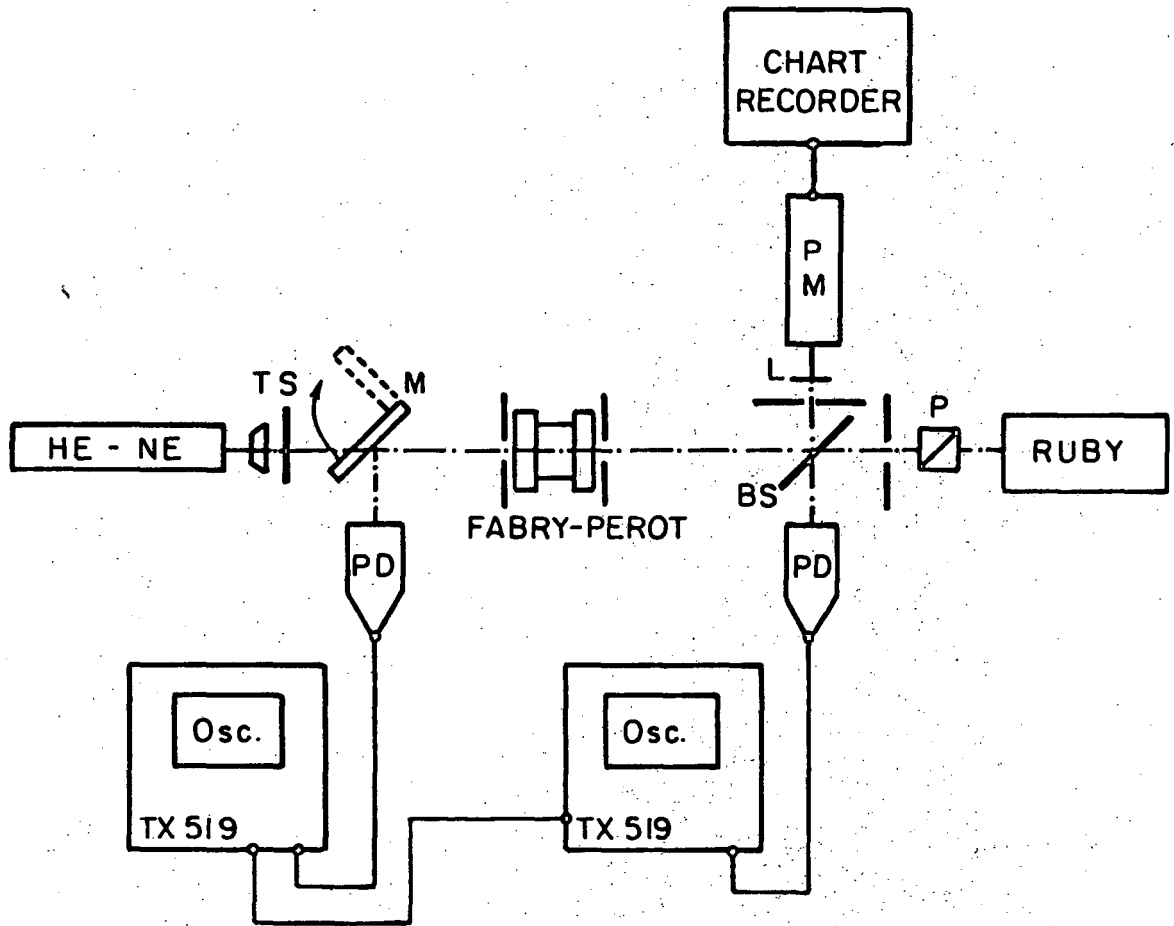
Figure Captions

- Fig. 1 Schematic diagram of the experimental setup. P: polarizer; BS: beamsplitters; L: lense; M: movable mirror; TS: telescope; PD: photodiode; PM: photomultiplier.
- Fig. 2 $I_{in}(t)$, $I_{out}(t)$, $\Delta\phi(t)$, and I_{out} vs. I_{in} for $t_R < \tau_p \ll \tau_D$ with $t_R = 0.11$ nsec, $\tau_p = 14$ nsec, and $\tau_D = 145$ nsec. The FP cavity is filled with MBBA. The curves are calculated from Eqs. (1), (4), and (7), while the dots are obtained from measurements. Three modes of operation are presented here, (a) power limiter, (b) differential gain, and (c) bistability.
- Fig. 3 $t_R < \tau_p < \tau_D$ with $t_R = 0.11$ nsec, $\tau_p = 62$ nsec, and $\tau_D = 145$ nsec. Others are the same as Fig. 2.
- Fig. 4 $t_R < \tau_p \approx \tau_D$ with $t_R = 0.11$ nsec, $\tau_p = 14$ nsec, and $\tau_D = 15$ nsec. Others are the same as in Fig. 2.
- Fig. 5 $t_R < \tau_D < \tau_p$ with $t_R = 0.11$ nsec, $\tau_p = 62$ nsec, and $\tau_D = 15$ nsec. Others are the same as Fig. 2.
- Fig. 6 $\tau_D < t_R < \tau_p$ with $t_R = 0.10$ nsec, $\tau_p = 14$ nsec, and $\tau_D = 45$ psec. The FP cavity is filled with nitrobenzene. Others are the same as in Fig. 2.
- Fig. 7 $\tau_D \ll t_R < \tau_p$ with $t_R = 0.11$ nsec, $\tau_p = 14$ nsec, and $\tau_D = 2$ psec. The FP cavity is filled with CS_2 . Others are the same as in Fig. 2.
- Fig. 8 $\tau_D \ll t_R < \tau_p$ with $t_R = 0.11$ nsec, $\tau_p = 62$ nsec, and $\tau_D = 2$ psec. The FP cavity is filled with CS_2 . Others are the same as in Fig. 2.
- Fig. 9 $I_{in}(t)$, $I_{out}(t)$, and I_{out} vs. I_{in} of the bistable mode of opera-

tion calculated for three different pulse durations τ_p with $\Delta\phi_0 = -0.4\pi$, $\tau_D = 0.01 t_R$, $R_\alpha = 70\%$, and the normalized input peak intensity kept constant. Note the different time scales in the figures on the left.

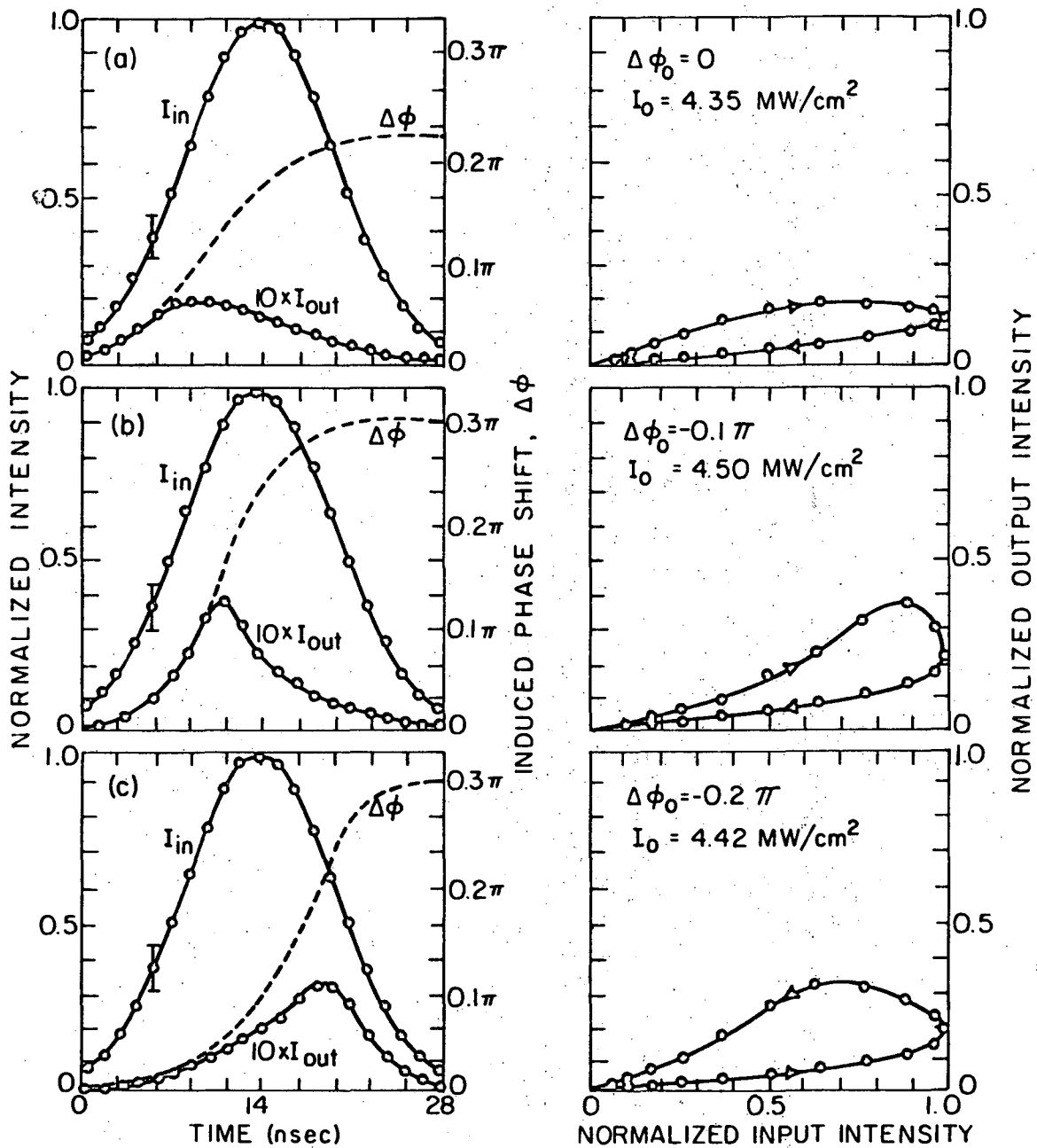
Fig. 10 $I_{in}(t)$, $I_{out}(t)$, and I_{out} vs. I_{in} of the bistable mode of operation for three different molecular relaxation times τ_D with $\Delta\phi_0 = -0.4\pi$, $\tau_p = 250 t_R$, $R_\alpha = 70\%$, and the input peak intensity kept constant.

Fig. 11 $I_{in}(t)$, $I_{out}(t)$, and I_{out} vs. I_{in} of the bistable mode of operation for three different effective mirror reflectivities R_α with $\Delta\phi_0 = -0.4\pi$, $\tau_D = 0.01 t_R$, $\tau_p = 250 t_R$, and the input peak intensity kept constant.

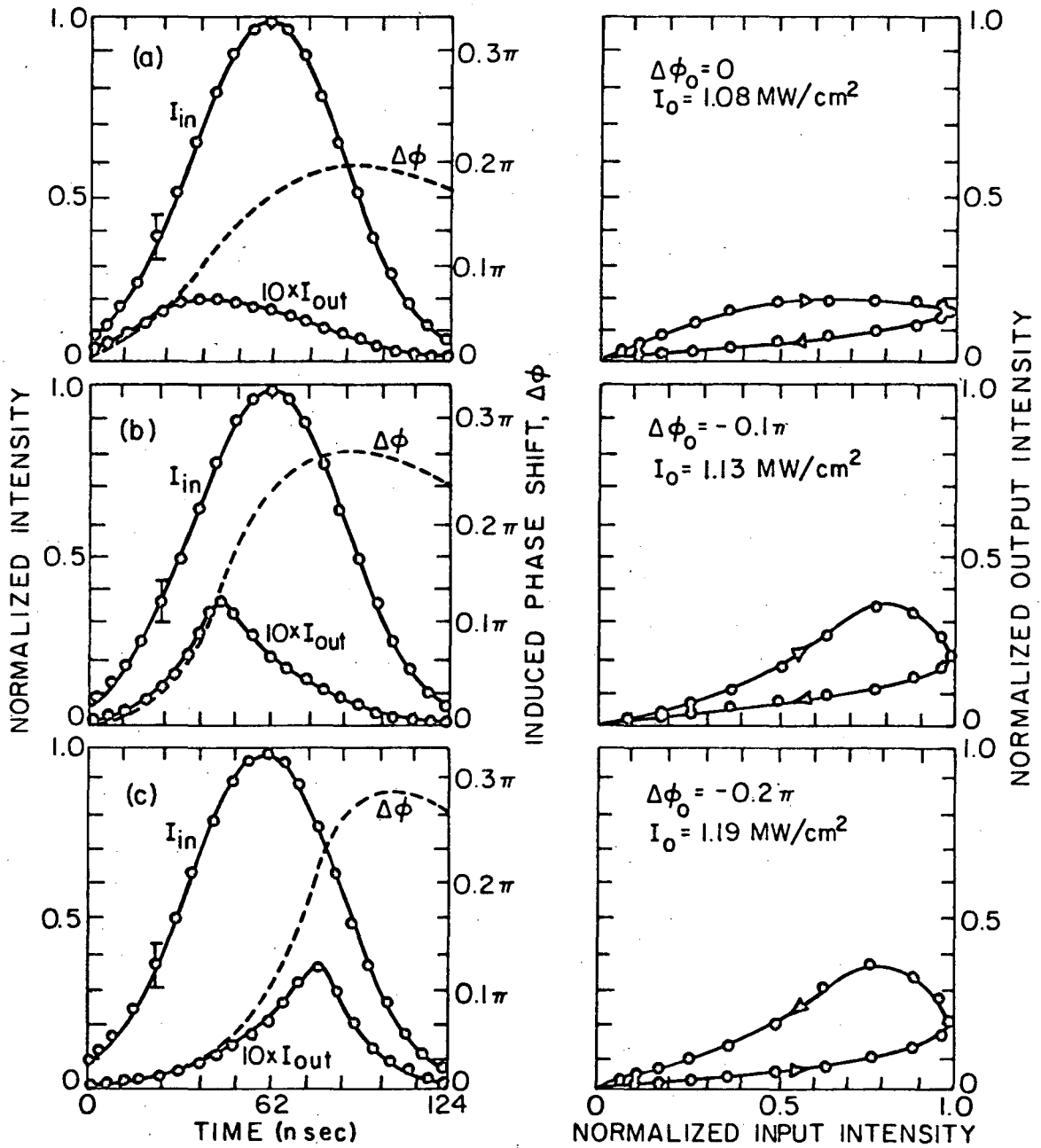


XBL 789-5795

Fig. 1

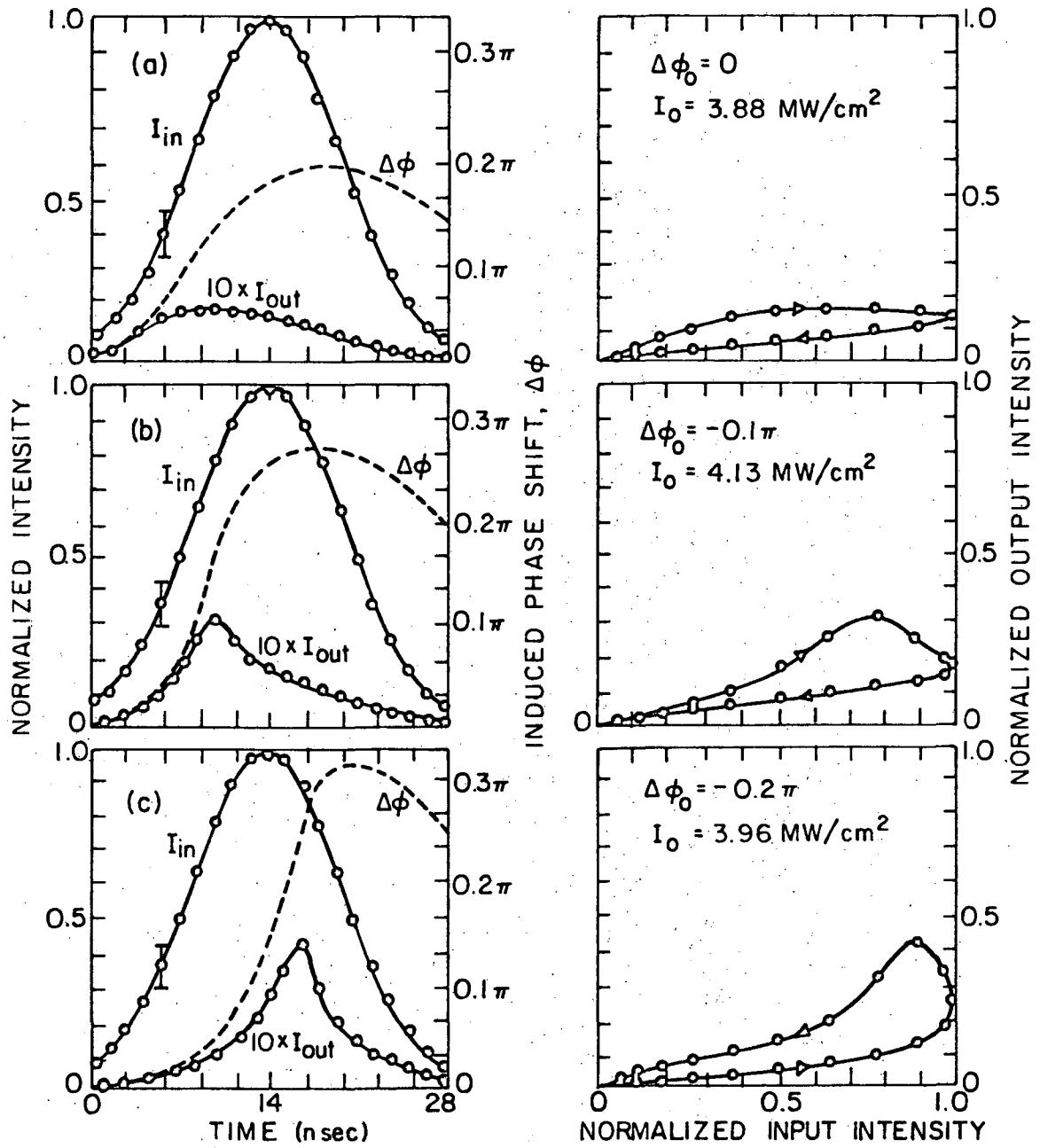


XBL 789-5799

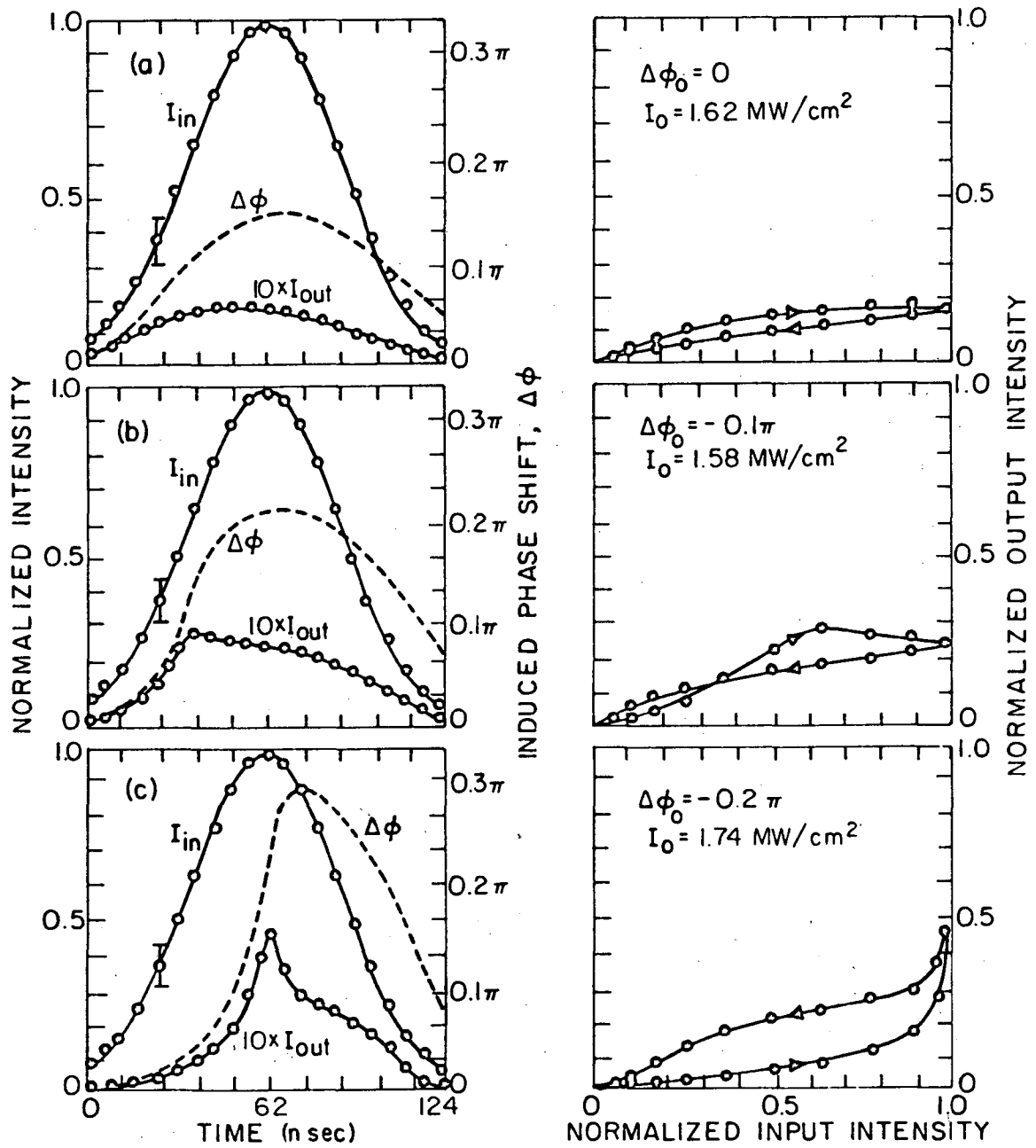


XBL789-5800

Fig. 3

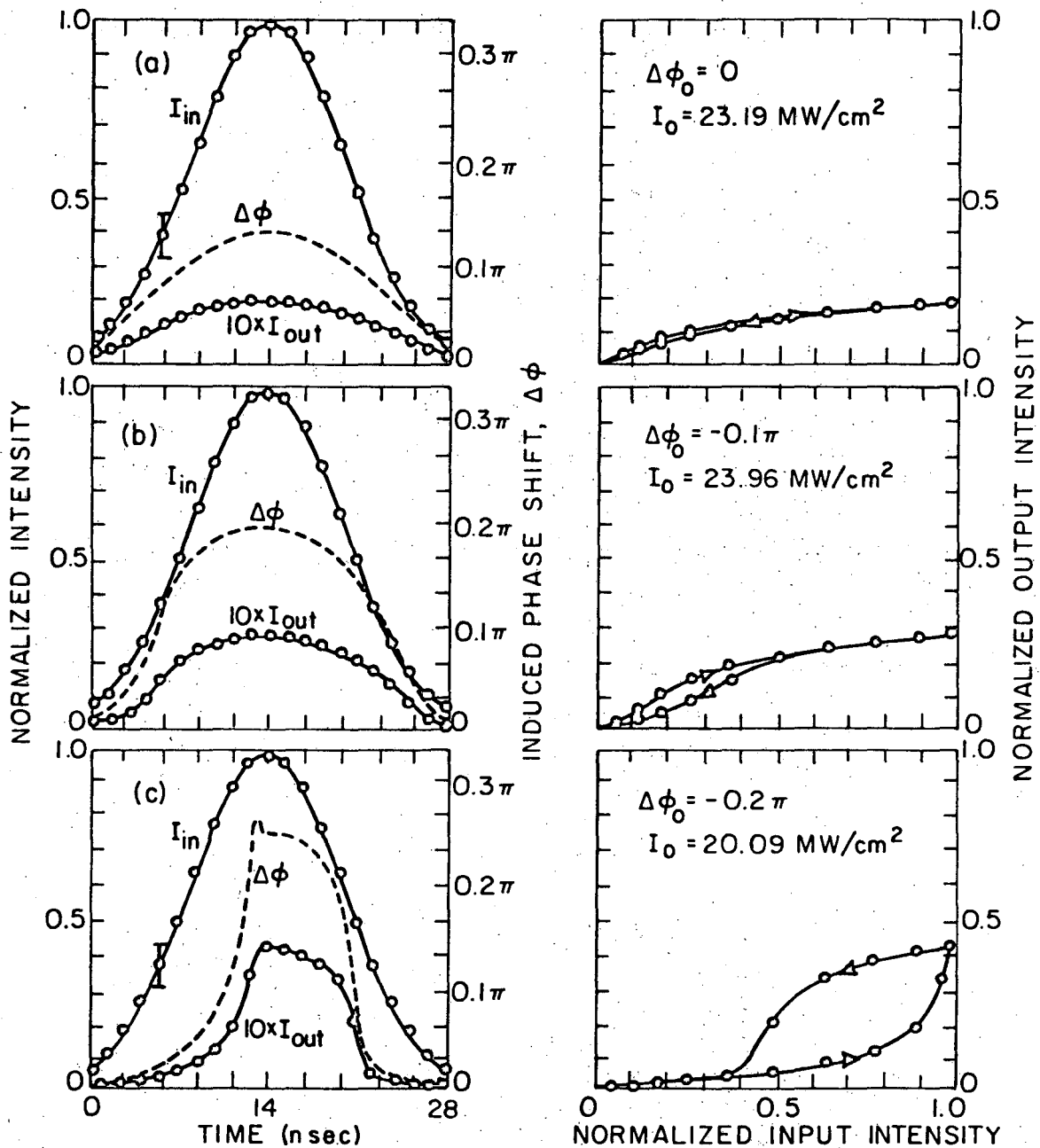


XBL789-5801



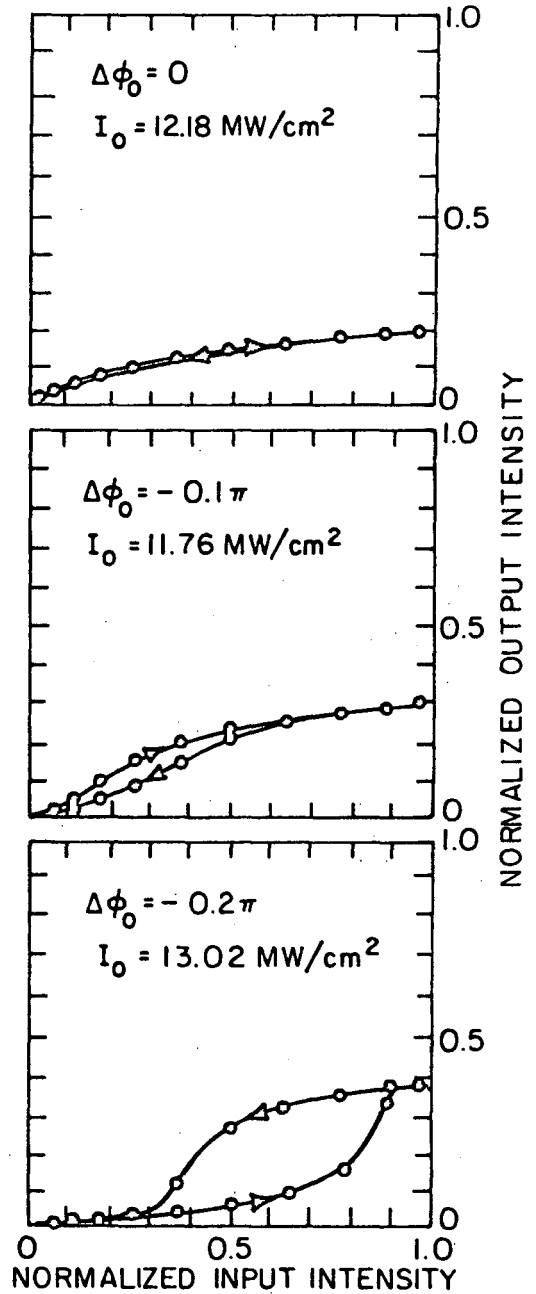
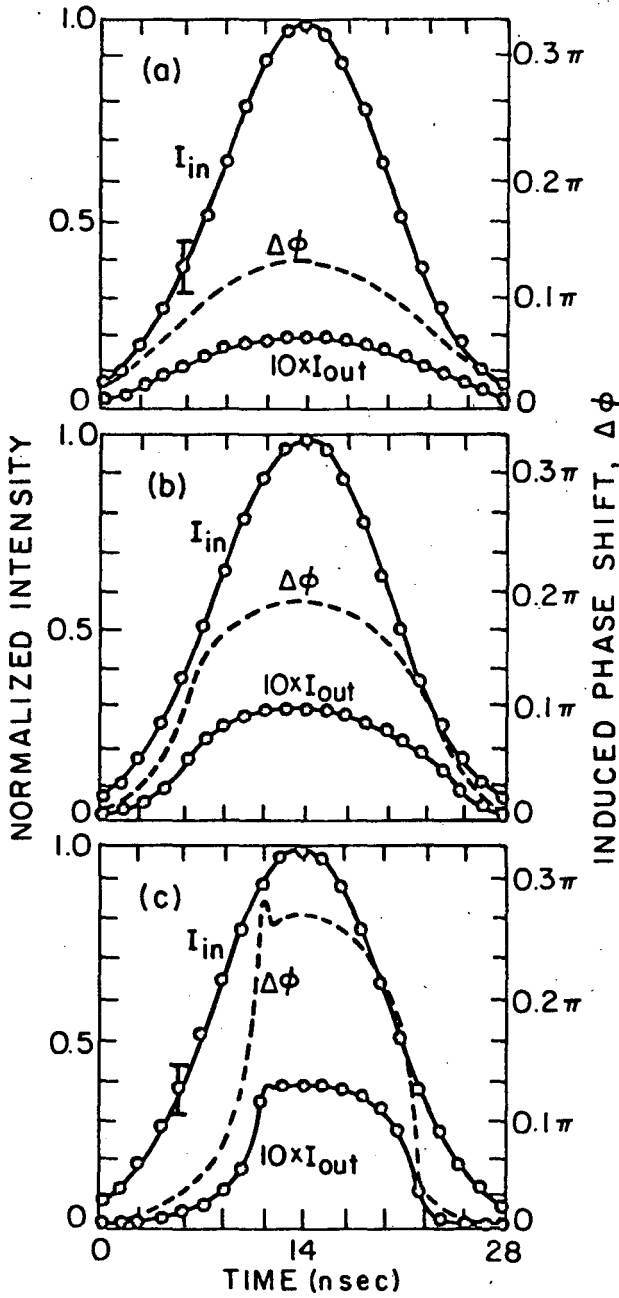
XBL789-5802

Fig. 5

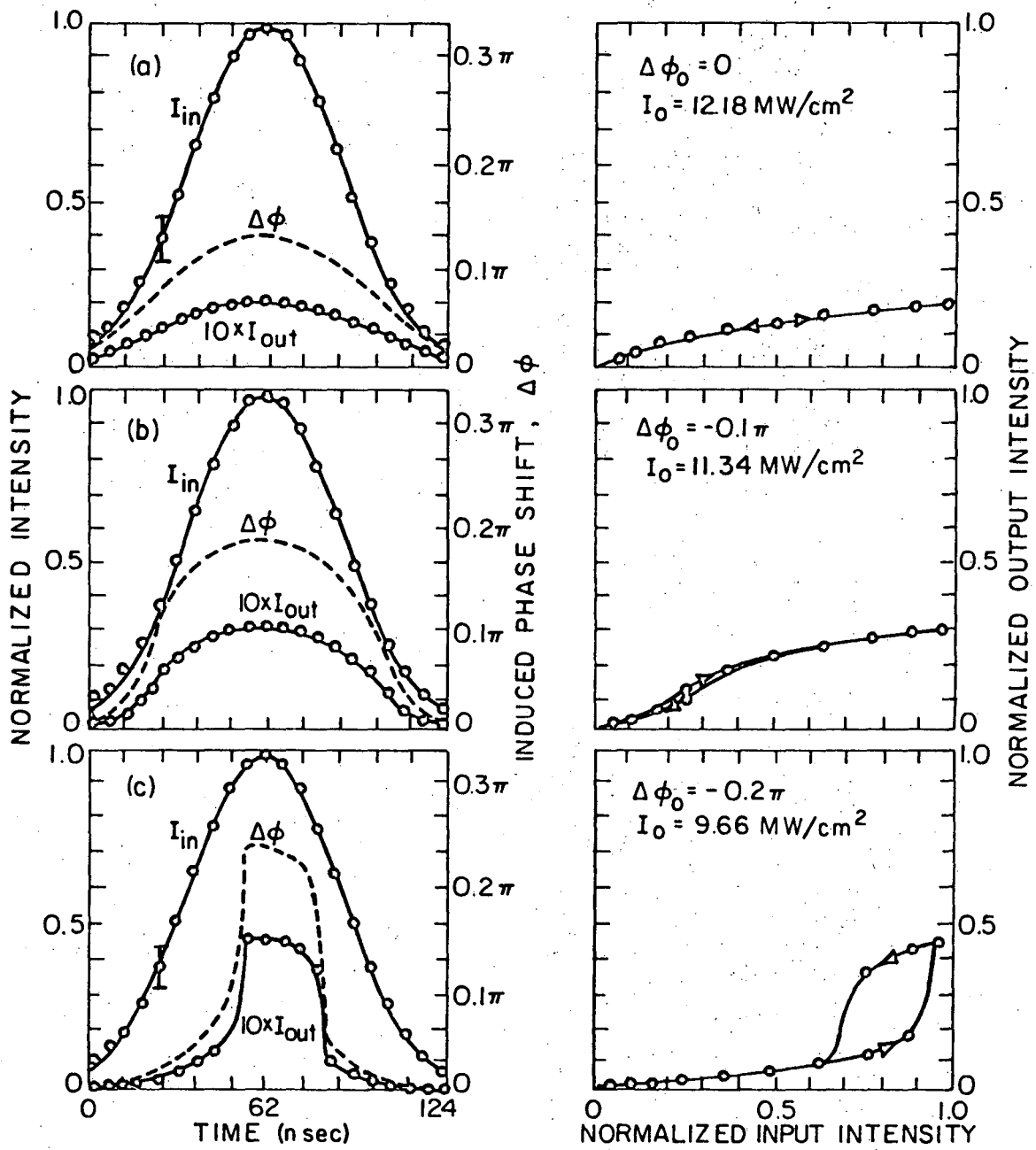


XBL 789-5803

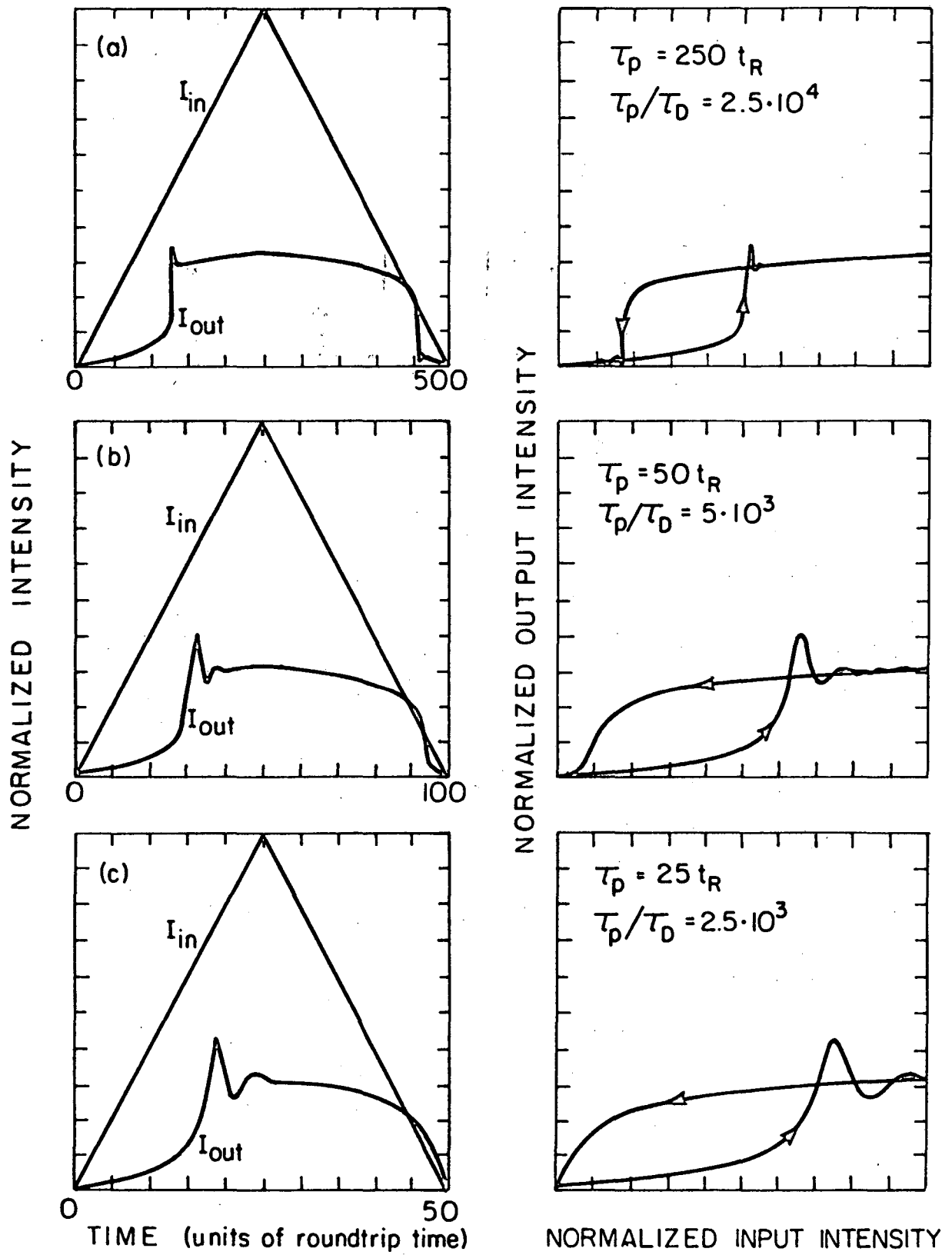
Fig. 6



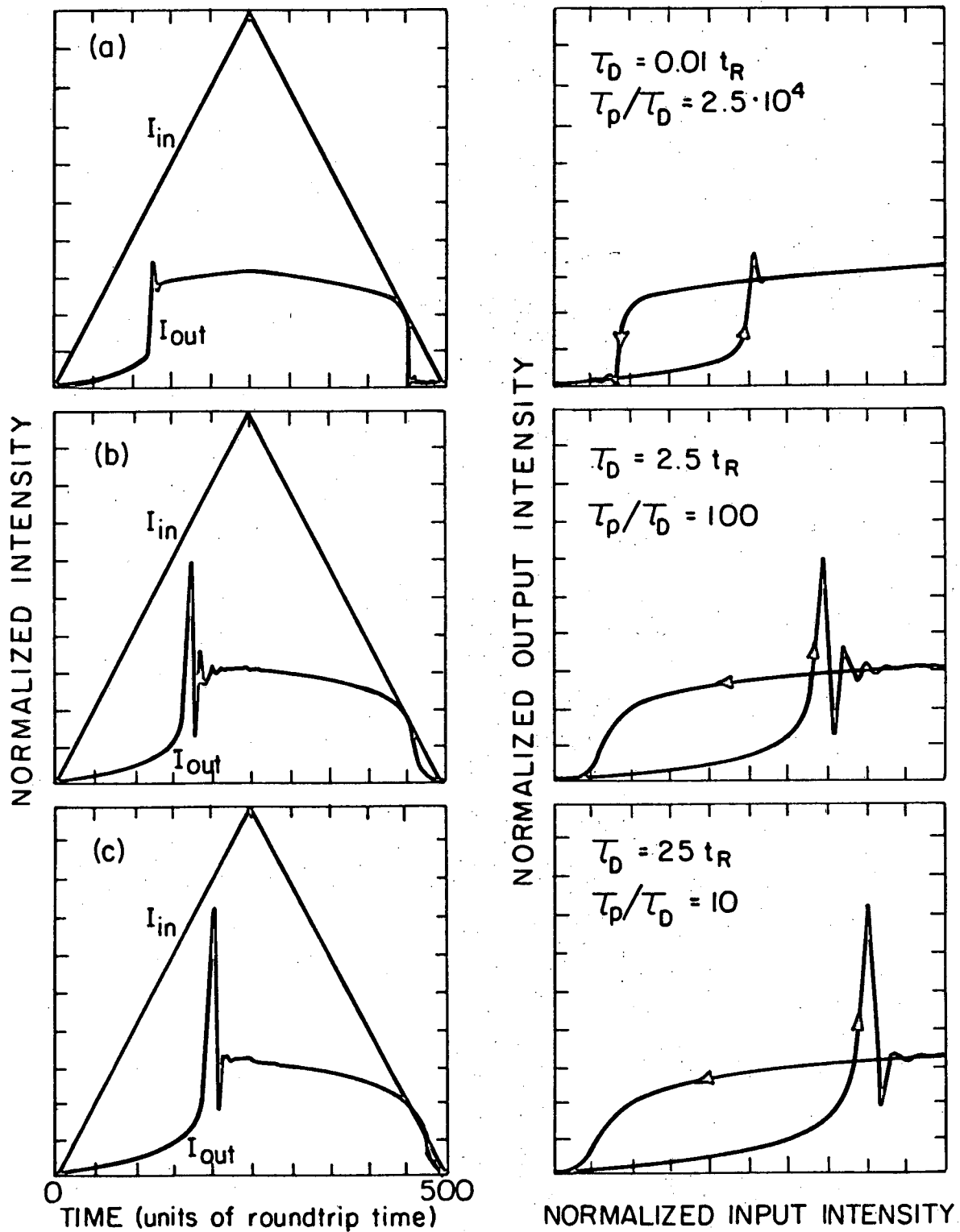
X BL789-5804



XBL789-5805

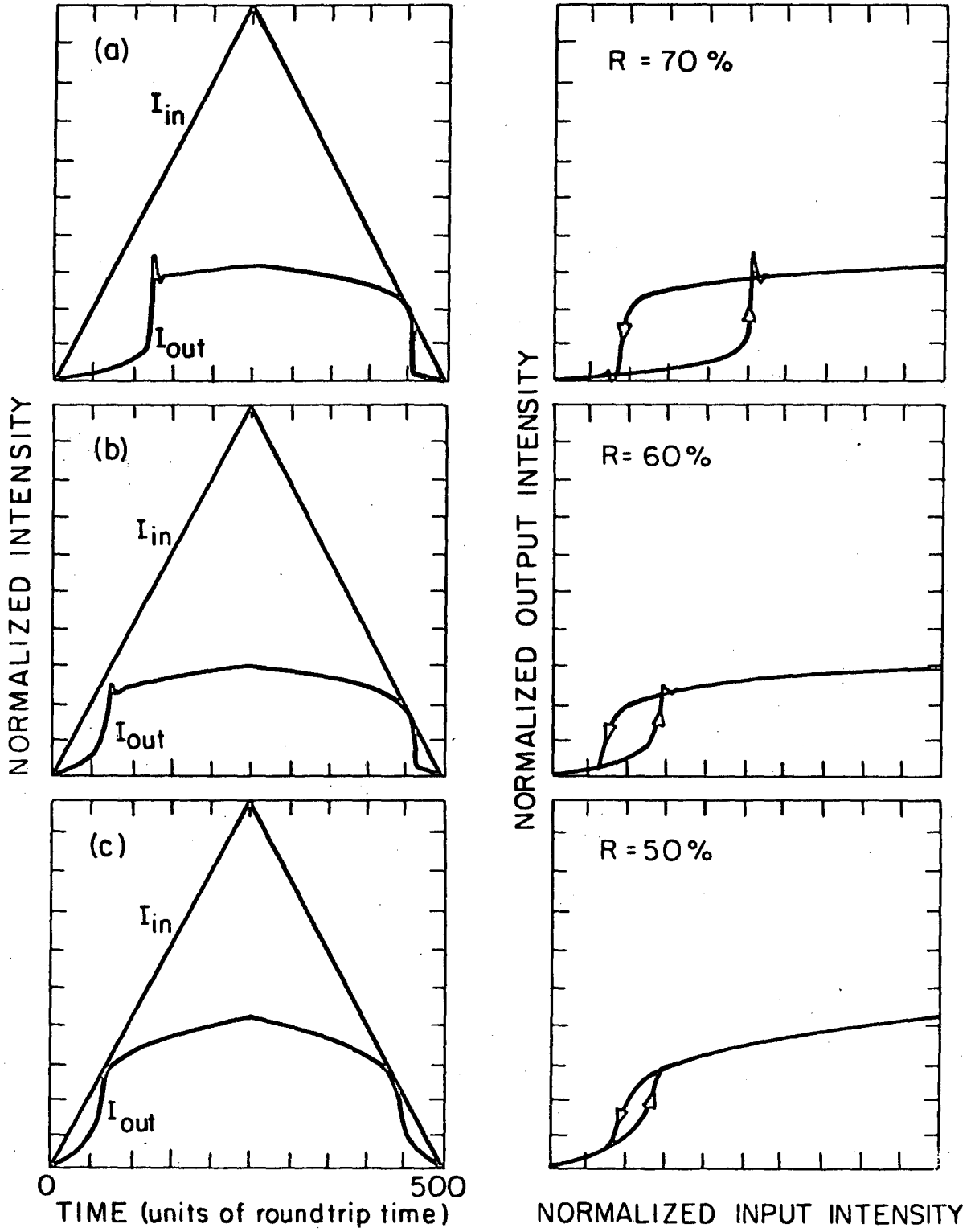


XBL789-5796



XBL 789-5797

Fig. 10



XBL 789-5798

Fig. 11

This report was done with support from the Department of Energy. Any conclusions or opinions expressed in this report represent solely those of the author(s) and not necessarily those of The Regents of the University of California, the Lawrence Berkeley Laboratory or the Department of Energy.

TECHNICAL INFORMATION DEPARTMENT
LAWRENCE BERKELEY LABORATORY
UNIVERSITY OF CALIFORNIA
BERKELEY, CALIFORNIA 94720